A Comparison of Control Techniques for Robust Docking Maneuvers of an AGV

Article *in* Control Systems Technology, IEEE Transactions on · July 2012

DOI: 10.1109/TCST.2011.2159794 · Source: IEEE Xplore

CITATIONS
72

READS
970

2 authors:

Jorge Villagra
Spanish National Research Council
43 PUBLICATIONS **1,486** CITATIONS
SEE PROFILE

David Herrero-Perez
Universidad Politécnica de Cartagena
59 PUBLICATIONS **1,106** CITATIONS
SEE PROFILE

A Comparison of Control Techniques for Robust Docking Maneuvers of an AGV

Jorge Villagra and David Herrero-Pérez

***Abstract*—This work addresses the path tracking problem of industrial guidance systems used by automated guided vehicles (AGVs) in load transfer operations. We focus on the control law that permits to AGVs to operate tracking a predefined route with industrial grade of accuracy, repeatability and reliability. One of the main issues of this problem is related to the important weight variation of AGVs when transporting a load, which induces slipping and skidding effects. Besides, localization error of the guidance system should be taken into account because position estimation is typically performed at a low sample rate. Other key point is that control law oscillations can knock down the load, which gives rise to safety and performance problems. Three control techniques—fuzzy, vector pursuit and flatness-based control—are compared in order to evaluate how they can deal with these problems and satisfy the robustness requirements of such an industrial application.**

***Index Terms*—Automated guided vehicles (AGVs), flatness control, fuzzy control, nonlinear robust control, vector pursuit.**

I. Introduction

NOWADAYS, the last generation of automated guided vehicles (AGVs) systems [1], [2] incorporates wireless guidance systems, using laser or inertial sensors, that permit to locate these vehicles with the precision needed for performing accurate maneuvers. However, popular commercial industrial navigation systems, namely laser navigation ones, induce problems related to the low pose estimation rate. This problem is usually solved by fusing those position estimations with odometry information, whether from wheel encoders or from inertial sensors. Nevertheless, the position estimation rate is still relatively low, which represents a key point that the tracking technique should take into account.

The typical load transfer operations of AGV systems consist of pick-up and delivery services between pick-up/delivery stations. In order to do so, the AGV should navigate between stations performing precise docking maneuvers to pick-up or deliver the transport load. Navigation between stations is referred as point-to-point navigation whereas precise maneuvers are referred as docking operations. The docking maneuvers need higher accuracy than navigation tasks because the vehicle can collide against the station/load or knock down the load due to an inaccurate maneuver. Hence, slight errors in docking maneuvers can damage the load, the station, and the vehicle.

Manuscript received January 04, 2011; accepted June 05, 2011. Manuscript received in final form June 10, 2011. Date of publication July 18, 2011; date of current version May 22, 2012. Recommended by Associate Editor M. Mattei.

J. Villagra is with the Center for Automation and Robotics, Spanish National Research Council (CSIC), Arganda del Rey, Madrid 28500, Spain (e-mail: jorge.villagra@iai.csic.es).

D. Herrero-Pérez is with the Structures and Construction Department, Technical University of Cartagena, Cartagena 30202, Spain (e-mail: david.herrero@upct.es).

Color versions of one or more of the figures in this paper are available online at http://ieeexplore.ieee.org.

Digital Object Identifier 10.1109/TCST.2011.2159794

This work is focused on docking operations, which should satisfy robustness constraints, given the industrial nature of this application, to avoid the problems mentioned above. Moreover, the docking operations should be performed as fast as possible avoiding vibrations induced by eventual high jerk variations in control actions. These vibrations result critical for both the accuracy of the docking operation and for the stability of the load. A comparison of path tracking techniques focused on reducing jerk variations is performed in order to minimize the vibration effects. Besides, the complexity and time consuming for on-site startup is also considered.

A. Non-Model-Based Control Approaches

The application of linear control methods in wheeled mobile robots (WMR) is well reported in the literature [3]. However, AGVs are characterized by nonlinear dynamics and affected by an important number of disturbances, such as turning and static friction or variations in the amount of cargo.

The complexity of AGV dynamics, the difficulty of obtaining the actual vehicle parameters, the variability of certain model parameters and the human-knowledge available on speed and steering control have traditionally motivated the use of soft computing paradigms, such as fuzzy logic [4], [5], neural networks [6] or even adaptive techniques inspired on biological immune systems [7]. Fuzzy logic emulates the human reasoning process with its capacity to deal with imprecision and uncertainty. However, it aims to minimize both the position and heading errors, normally by some kind of weighting function, with no corresponding geometrical meaning.

Vector pursuit controllers [8] not only provide a way to move the AGV to a certain position, but also with a given heading and curvature. However, a look-ahead distance should be defined, which is of paramount importance due to the precision needed in docking operations. In this respect, even if vector pursuit control for AGVs can provide remarkable tracking results when compared to other non-model-based control techniques, the following two main issues are likely to be improved.

- Determinism is much harder to obtain than with any model-based technique. Consequently, some tracking quality indicators, as jerk variations or time to docking point, are difficult to be imposed *a priori*.
- Since the choice of look-ahead distance significantly influences the closed-loop behavior, flexibility and ease of reconfiguration cannot be guaranteed.

B. Model-Based Control Approaches

Even though WMR model based control problems have been intensively studied in recent years (cf. [9] and the references therein), most existing works assume, on the one hand, that they satisfy non-slipping and non-skidding conditions, and on the other hand, that high sample rate measurements are available. However, these assumptions are hardly ever fulfilled, and

therefore stability domains and control performance can be significantly altered.

Several solutions have been proposed in order to compensate the effects induced by uncertainty and/or neglected dynamics, such as model-based adaptive control [10]–[12], singular perturbations [13], sliding mode control [14], or Lyapunov-based control [15]. Most of these approaches need a good knowledge of the unmodeled dynamics or suffer from robustness to demanding disturbances (which are arbitrarily constrained to unrealistic bounds).

Besides, an important issue in AGV control is that not only a good path tracking should be assured, but it is also desirable a good behavior in terms of jerk. The latter is concerned with the ability to safely dock, undock and carry the pallets, and consequently, with the amount of material that can be handled in a single trip.

Flatness-based control [16] turns out to be a very interesting tool because it allows to take advantage of WMRs flat structure to simply generate open-loop control to follow the path. Moreover, a feedback control can be naturally introduced so that time dependence is decoupled from the geometric task. To the best of our knowledge, only [17] has coupled flatness-based control with robust control techniques (sliding modes, to be specific). However, these methods can be constrained by mechanical issues due to highly switching control actions. Recently, [18] proposed a dynamic extension of classical flatness results by introducing a velocity-scheduling. Unfortunately, neither the beforehand mentioned disturbances nor unmodeled low-level dynamics are taken into account. For all these reasons, a novel control approach, called intelligent PID (i-PID), will be used to improve the dynamic behavior under a high degree of uncertainty.

As aforementioned, we assume that AGV position estimation rate is relatively low (resulting of fusing laser navigation sensor and odometry). Few model-based control techniques take into account such kind of limitations, and when they are explicitly treated [19], supplementary sensors are considered.

All these challenging conditions will be used in simulations to compare the performance of this control approach.

To sum up, the main contributions of our work are as follows:

- to compare control philosophies (intelligent control, geometric vector pursuit or nonlinear model-based control) that are rarely confronted for a real application;
- to consider a realistic WMR model, where not only slipping and skipping are taken into account, but also traction and steering dynamics;
- to enlarge robustness properties of the approach introduced by [20] with a control strategy that guarantees low jerk variations.

C. Outline

Section II is devoted to how traction and steering dynamics and slipping and skidding effects can naturally be added to the classical kinematic model. Fuzzy and vector pursuit control are briefly recalled in Section III. Flatness-based control is introduced in Section IV. Since flatness-based control presents poor robustness properties to neglected dynamics or disturbances an intelligent feedback control is added in Section IV-A.

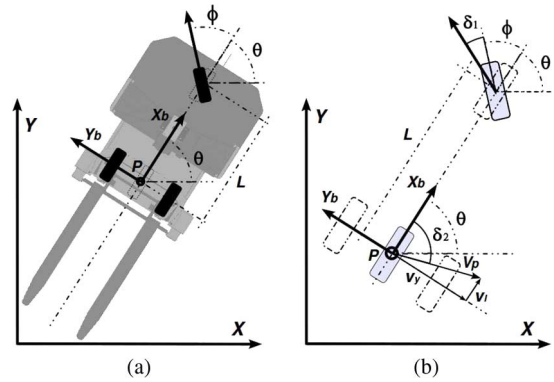

Fig. 1. (a) Purely kinematic WMR and (b) skidding and slipping WMR.

Section V shows, through simulation results, the advantages of this new technique with respect to fuzzy, vector pursuit and more standard flatness-based controllers. Finally, some concluding remarks are discussed in Section VI.

II. Wheeled Mobile Robot Model: From Kinematics Towards Skidding and Slipping

A. Pure Kinematic Model

The WMR considered in this paper, shown in Fig. 1(a), has a body frame $\{X_b, Y_b\}$ attached to the reference point P with coordinates $\xi = [x, y]^T$ in global coordinate frame $\{X, Y\}$. The θ value denotes the orientation of the basis $\{X_b, Y_b\}$ with respect to the global frame, so that the generalized coordinates of the WMR are $q = (x, y, \theta)$. The robot is equipped with a front-centered steerable wheel (whose angle is represented by ϕ) and fixed parallel rear wheels. The resulting state-space kinematic model can be written as follows:

$$\begin{bmatrix} \dot{x} \\ \dot{y} \\ \dot{\theta} \end{bmatrix} = \begin{bmatrix} v\cos\theta \\ v\sin\theta \\ \frac{v}{L}\tan\phi \end{bmatrix}. \tag{1}$$

B. Skidding and Slipping Model

1) Slipping: Under pure rolling assumption, where there is no tire deformation, the wheel's linear velocity is $v_l = r\omega$ with r and ω the wheel radius and angular speed, respectively. However, this is not the case when an important acceleration is applied to the vehicle. The wheel slipping can be characterized by slip ratio $\tau \in [-1, 1]$

$$\begin{cases} \tau = \frac{\omega r - v_l}{v_l}, & \text{if } v_l > \omega r, v_l > 0 \\ \tau = \frac{\omega r - v_l}{\omega r}, & \text{if } v_l < \omega r, \omega r > 0. \end{cases}$$

Equivalently, a longitudinal slip velocity can be defined as $d = r\omega - v_l$, that can be explicitly expressed in terms of load and friction conditions [21].

2) Skidding: When a turning maneuver begins, a cornering force acts laterally on the wheel's contact patch, causing the wheel to transverse along a direction away from the wheel's plane. This behavior is referred as skidding. The angle between the wheel's direction of travel and the wheel's plane is known as the slip angle δ.

Consider that the fixed parallel wheels can be simplified by a fictitious wheel at the center of those parallel wheels (see Fig. 1). Denote V_P as the velocity of the reference point P; v_y denotes the projection of velocity V_P on axis Y_b, and v_l represents the beforehand mentioned linear wheel's velocity, which is the velocity V_P projected on X_b. These two velocities (v_l, v_y) are related to the slip angle δ by the geometrical relationship $\tan\delta = v_y/v_l$.

Fig. 1(b) shows the motion of the AGV using a WMR model in the presence of skidding and slipping, where ϕ denotes the robot front steering angle, δ_2 represents the generalized slip angle of the rear fictitious wheel and δ_1 the slip angle of the front wheel. Lateral velocity v_y is modeled as the output of a second order linear system whose input is steering angle (see [22] for further details)

$$V_y(s) = \frac{K_s\omega_s^2}{s^2 + 2\eta_s\omega_s + \omega_s^2}\Phi(s) \tag{2}$$

where K_s, η_s, and ω_s are the lateral velocity (skidding) static gain, damping ratio and undamped natural frequency, respectively.

We extend the equation formulation used in the ideal cases (1) in order to derive the WMR model under these assumptions to the situations with skidding and slipping (see [23] for more details)

$$\begin{bmatrix} \dot{x} \\ \dot{y} \\ \dot{\theta} \end{bmatrix} = \begin{bmatrix} v_l\cos\theta - v_y\sin\theta \\ v_l\sin\theta + v_y\cos\theta \\ \frac{v_l}{L}\tan(\phi+\delta_1) - \frac{v_y}{L} \end{bmatrix} \tag{3}$$

with control variables $u = r\omega$ and ϕ.

C. Electrical Traction and Steering Dynamics

A first order model has been considered in order to model the powered steering and the mechanical transmission to the front wheel. Concerning the electrical traction system, a dead-time has to be added to a second order model to take into account special H-Bridge protection systems. Following [24] traction and steering dynamics can be modeled as follows:

$$\begin{aligned} V_r(s) &= \frac{K_v\omega_v^2}{s^2 + 2\eta_v\omega_v s + \omega_v^2}e^{-\tau_v s}V(s) \\ \Phi_r(s) &= \frac{K_\phi\omega_\phi}{s+\omega_\phi}\Phi(s) \end{aligned} \tag{4}$$

where K_v and K_ϕ are the velocity and steering angle static gains, ω_v and ω_ϕ are the velocity and steering angle natural frequencies, η_v is the velocity damping factor, τ_v is the traction system delay, and $V_r(s)$, $V(s)$, $\Phi_r(s)$, and $\Phi(s)$ are the actual and desired velocities, and the real and desired steering angle (in Laplace domain), respectively.

III. Non-Model-Based Control Approaches

The complexity of AGV dynamics and the difficulty of obtaining the actual vehicle dynamic parameters have motivated the use of two non-model-based control approaches. Both methods make use of a point, belonging to the path to follow, in front of the AGV, which is calculated by the so-called look-ahead distance, to calculate the wheel speed and steering angle.

A. Fuzzy Control

Fuzzy control systems use a kind of approximate reasoning that resembles the decision-making process of humans. Because the solution to the problem addressed can be formulated in terms that human operators can understand, their experience can be used in the design of the controller. However, the process to obtain fuzzy knowledge base from an expert is often based on a tedious and unreliable trial and error approach, and therefore, different techniques have been used for the automated design and optimization of fuzzy logic controllers [25].

The proposed solution is based on a Mamdani-type [26] fuzzy controller, which consists of a collection of N fuzzy rules where each one is composed of a set of n fuzzy numbers (antecedent) and m real parameters (consequent). The antecedents are trapezoidal fuzzy sets that can be characterized using four parameters and the output fuzzy singletons using only one number for each one. The rules of the fuzzy controller are as follows:

$$\text{IF} \quad \phi \in A \quad \text{THEN} \quad \omega = c0,\ v = c1$$

where the input fuzzy set ϕ represents the heading to the current look-ahead point in the trajectory (antecedent) and the two output crisp values, ω and v, represent the angular and linear control variables, respectively (consequents). The angular velocity ω is related to the steering angle ϕ by $\omega = v\tan\phi/L$. The membership functions are fixed and known in advance, besides, their sum is one. The fuzzy knowledge-base is composed of seven trapezoidal membership functions for the input fuzzy variable, which are labeled as NL (negative large), NM (negative medium), NS (negative small), Z (zero), PS (positive small), PM (positive medium), and PL (positive large). There are seven values for the angular velocity that are denoted by the same labels. Finally, there are four values for the linear velocity that are labeled by Z (zero), S (small), M (medium), and F (full). The fuzzy controller is composed of seven rules obtained heuristically

$$\begin{aligned} &\text{IF} \quad \phi \in NL \quad \text{THEN} \quad \omega = NL,\ v = Z \\ &\text{IF} \quad \phi \in NM \quad \text{THEN} \quad \omega = NM,\ v = S \\ &\text{IF} \quad \phi \in NS \quad \text{THEN} \quad \omega = NS,\ v = M \\ &\text{IF} \quad \phi \in Z \quad \text{THEN} \quad \omega = Z,\ v = F \\ &\text{IF} \quad \phi \in PS \quad \text{THEN} \quad \omega = PS,\ v = M \\ &\text{IF} \quad \phi \in PM \quad \text{THEN} \quad \omega = PM,\ v = S \\ &\text{IF} \quad \phi \in PL \quad \text{THEN} \quad \omega = PL,\ v = Z. \end{aligned}$$

We have to remark that the heading to look-ahead point is the input of the fuzzy controller, which depends on look-ahead distance and trajectory to follow.

B. Vector Pursuit

The vector pursuit approach [8] is a geometric path tracking (pure pursuit) method that employs both distance and heading to some goal position (look-ahead) to calculate the curvature to move a vehicle from its current position to such a goal.

The Screw Theory is used in vehicle control problem as follows. First, two instantaneous screws are calculated: $\vec{S}_t$ that accounts for the translation from vehicle's location to look-ahead

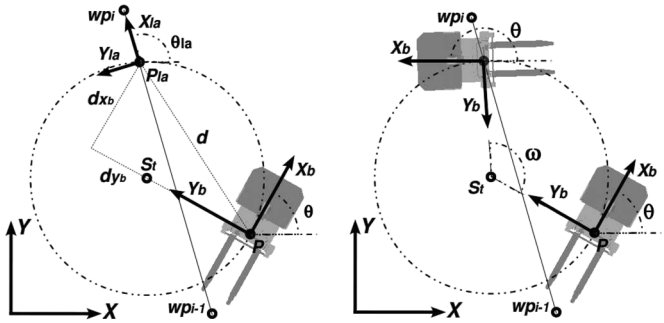

Fig. 2. Instantaneous screw $\vec{S}_t$: (a) translation from the current AGV location to the look-ahead position and (b) the rotation defined by this screw.

position and $\vec{S}_r$ that accounts for the rotation from vehicle's location to the desired orientation. Then, the screw $\vec{S}_d$ that accounts for the instantaneous vehicle's motion is calculated. This instantaneous screw depends on $\vec{S}_t$ and $\vec{S}_r$ screws, and it is easily obtained making use of the additive property of screws. Finally, the wheel speed and wheel angle generating the motion along the resulting screw are used to reach the look-ahead point in such an instant.

The proper selection of $\vec{S}_t$ and $\vec{S}_r$ screws is a key point because they should be located taking into account some constraints, such as maximum curvature of nonholonomic platforms. Consider the robot has the body frame $\{X_b, Y_b\}$ with coordinates (x, y, θ) in the global coordinate system $\{X, Y\}$ specified in Section II. Let d be the vector from robot's location to the local target (look-ahead point) that the AGV should follow, and (dx_b, dy_b) the projection of vector d on the axes of robot coordinate system $\{X_b, Y_b\}$. This look-ahead vector d is obtained by the intersection of the route to follow and a circle of radius $|d|$ centered in the robot's frame $\{X_b, Y_b\}$. Fig. 2(a) shows two way-points, wp_i and wp_{i-1}, of the route to follow and the instantaneous look-ahead vector calculated to track such a route. The aim is moving the vehicle from its current location to the coordinates $(x_{la}, y_{la}, \theta_{la})$ depicted in Fig. 2(a), which axis x_{la} is parallel to the line-segment linking two way-points, and hence, tangent to the trajectory to follow.

The screw $\vec{S}_t$ is located at the center of a circumference that passes through both poses and that is tangent to the vehicle heading. The radius of circumference determines the curvature that vehicle should follow, which results so useful in order to satisfy the nonholonomic constraints of tricycle drive. Thus, $\vec{S}_t$ screw is defined to satisfy

$$S_t = \left[\frac{d^2}{2dy_b} \cos\theta + y, \frac{d^2}{2dy_b} \sin\theta - x \right].$$

The screw $\vec{S}_t$ represents the displacement from the vehicle's pose to the target position, shown in Fig. 2(b), rotating ω around the screw $\vec{S}_t$. The screw $\vec{S}_r$ is located at the robot's frame $\{X_b, Y_b\}$ in order to represent a pure rotation, which is used to reach the target heading θ_{la}. Thus, $\vec{S}_r$ is defined as $S_r = [y, -x]$. These screws, $\vec{S}_t$ and $\vec{S}_r$, are weighted with factors k_t and k_r in order to control their influence on the resulting screw $\vec{S}_d$. These factors, k_t and k_r, represent the angular velocities ω_t and ω_r applied to $\vec{S}_t$ and $\vec{S}_r$ screws, respectively. The angle ω that vehicle should rotate to reach the look-ahead point can be calculated using the expression

$$\omega = a\tan 2\left(2dy_b{}^2 - |d|^2, 2dx_b dy_b\right) - a\tan 2\left(\frac{d^2}{2dy_b}, 0\right).$$

The time to translate the vehicle to the look-ahead point is calculated as $t_t = \omega/\omega_t$, and the time to rotate the vehicle to the look-ahead bearing is calculated as $t_r = ((\theta_{la} - \theta) - \omega)/\omega_r$. Besides, a factor k is used to state the relationship between t_t and t_r as $t_r = kt_t$, where k is some positive constant greater than zero. Thus, the weighting factors can be determined as $k_t = \omega_t$ and $k_r = \omega_r$, where k_r can be derived to $k_r = \omega_t((\theta_{la} - \theta) - \omega)/k\omega$. Besides, the weighting factor satisfies $k = k_t/k_r$.

The coordinates (x_{S_d}, y_{S_d}) of resulting screw S_d in the global coordinate system $\{X, Y\}$ are determined by

$$\begin{aligned} x_{S_d} &= x - k\left(\frac{y_{la} - y}{\theta_{la} - \theta}\right) \\ y_{S_d} &= y + k\left(\frac{x_{la} - x}{\theta_{la} - \theta}\right). \end{aligned} \tag{5}$$

Finally, the coordinates $(x_{b_{S_d}}, y_{b_{S_d}})$ of resulting screw S_d in the vehicle's coordinate system $\{X_b, Y_b\}$ are used to calculate the movement of the vehicle to reach the look-ahead position

$$\begin{aligned} x_{b_{S_d}} &= (x - x_{S_d})\cos\theta + (y - y_{S_d})\sin\theta \\ y_{b_{S_d}} &= (y - y_{S_d})\cos\theta - (x - x_{S_d})\sin\theta \end{aligned} \tag{6}$$

where $x_{b_{S_d}}$ should be zero in order to satisfy the nonholonomic constraint of platform and $y_{b_{S_d}}$ should be greater than minimum turning radius of the tricycle drive.

The selection of look-ahead distance $|d|$ results of paramount importance because large look-ahead distances reduce the oscillations at the cost of increasing the position errors when high curvatures, while short look-ahead distances permit more accurate path tracking increasing the oscillations. Therefore, the choice of $|d|$ should be decided as a tradeoff between accuracy and robustness depending on the specific application.

IV. Flatness-Based Control

As shown in [16], the kinematic model of the WMR given in (1) is flat with flat outputs $z = \{x, y\}$. The three conditions above formulated to establish the flatness of a system can be verified in our case with the following expressions, which are easily obtained from (1):

$$\theta(t) = \arctan\left(\frac{\dot{y}(t)}{\dot{x}(t)}\right) \tag{7}$$

$$u(t) = \sqrt{\dot{x}^2(t) + \dot{y}^2(t)} \tag{8}$$

$$\phi(t) = \arctan\left(\frac{L\left(\dot{x}(t)\ddot{y}(t) - \ddot{x}(t)\dot{y}(t)\right)}{\left(\dot{x}(t) + \dot{y}(t)\right)^{3/2}}\right). \tag{9}$$

In order to avoid singularities of (7) and (9), [27] introduced a time-scaling tool, which may be interpreted as controlling the clock. To that end, a parameter change $t \mapsto \sigma(t)$ is applied, with σ an increasing function that represents the vehicle displacement profile.

As a result, a controller based on dynamic feedback linearization proposed by [27] is used to control the AGV. The compensator reads

$$\begin{aligned} \dot{v} &= \dot{\sigma}\left(v_1 \cos\theta_r(\sigma) - v_2 \sin\theta_r(\sigma)\right) \\ u &= v\dot{\sigma} \\ \phi &= \arctan\left(\frac{L}{v^2}\left(v_2 \cos\theta_r(\sigma) - v_1 \sin\theta_r(\sigma)\right)\right) \end{aligned} \tag{10}$$

where the dynamical extension variable v and inputs v_1, v_2 are such that the closed-loop system obtained from (1) and (10) is equivalent to a linear system, and more precisely to two chains of two integrators

$$\ddot{x}(t) = v_1(t) \qquad \ddot{y}(t) = v_2(t). \tag{11}$$

A linear feedback controller can be then designed to control this equivalent system

$$\begin{aligned} v_1 &= \ddot{x}_r + K_{D1}(\dot{x}_r - \dot{x}_e) + K_{P1}(x_r - x_e) \\ v_2 &= \ddot{y}_r + K_{D1}(\dot{y}_r - \dot{y}_e) + K_{P2}(y_r - y_e) \end{aligned} \tag{12}$$

where estimated position values x_e, y_e and their time derivatives have to be obtained from available measurements.

To achieve such stabilization, not only admissible reference trajectories have to be offline computed, but a speed profile $\dot{\sigma}(t)$ should also be provided.

A. Intelligent PID (i-PID) Control

The proposed time-scaling dynamic feedback guarantees a robust stabilization when initial conditions are not well known or soft disturbances are applied to the robot [27]. However, the convergence speed and the stability regions are significantly affected when important unmodeled dynamics or disturbances perturb the nominal behavior of the system.

To overcome this problem, an i-PID controller is used. The main advantage of this approach is that it uses a standard PID controller structure, but it is able to take into account, without any modeling procedure, the unknown parts of the system (see [28] and [29] for more details).

Consider a finite-dimensional multiple-input, multiple-output (MIMO) system, with m inputs $u = (u_1, \ldots, u_m)$ and n outputs $z = (z_1, \ldots, z_n)$

$$\Phi_j\left(z, \ldots, z^{(N_j)}, u, \ldots, u^{(M_j)}\right) = 0, \quad j = 1, \ldots, n.$$

If the assumption $\partial\Phi_j/\partial z_j^{(n_j)} \neq 0, j = 1, \ldots, n$ is verified, the implicit function theorem and a straightforward simplification (cf. [28]) locally yields

$$\begin{aligned} z_1^{(\mu_1)} &= F_1 + \alpha_{1,1}u_1 + \cdots + \alpha_{1,m}u_m \\ &\cdots \\ z_n^{(\mu_m)} &= F_n + \alpha_{n,1}u_1 + \cdots + \alpha_{n,m}u_m \end{aligned} \tag{13}$$

where $\alpha_{i,j}$, $i = 1, \ldots, n$, $j = 1, \ldots, m$ and μ_j, $j = 1, \ldots, m$ are non-physical constant parameters, which are chosen by the engineer with the following guidelines:

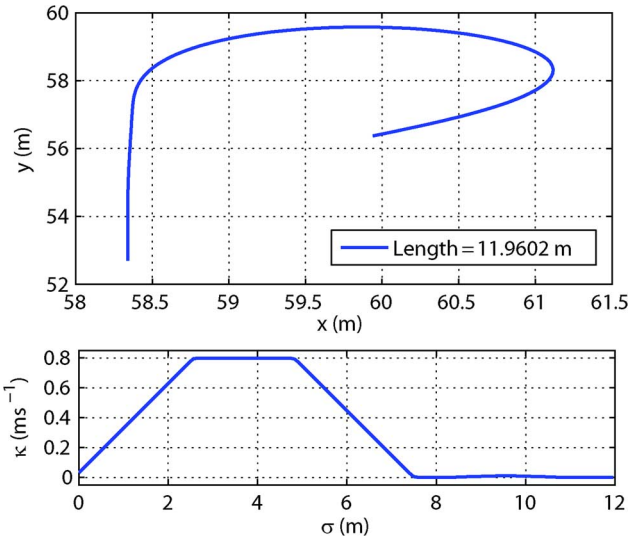

Fig. 3. Geometric path and its curvature in terms of the arc length.

- μ_m is an integer value (usually 1 or 2), which may represent the system degree, but not necessarily;
- $\alpha_{i,j}$ are chosen in such a way that F_j and $\alpha_{i,j}u_j$ are of the same magnitude.

Finally, F_j, $j = 1, \ldots, m$ are determined thanks to the knowledge of u_j, $\alpha_{i,j}$, and the estimates of $z_j^{(\mu_j)}$

$$F_j(t_k) = \hat{z}_j^{(\mu_j)}(t_k) - \sum_{i=1}^{m} \alpha_{j,i}u_i(t_{k-1}). \tag{14}$$

In fact, the F_j terms carry the whole information on the process to be controlled (which might include hardly identifiable parameters or complex time-varying phenomena, like frictions).

Feedback controller (11) permits to decouple the nonlinear model (1). This fact leads to a specially easy tuning of the MIMO i-PID, because the general model (13) yields for this specific case

$$\begin{aligned} x^{(\mu_1)}(t_k) &= F_1(t_k) + \alpha_1 v_1(t_{k-1}) \\ y^{(\mu_2)}(t_k) &= F_2(t_k) + \alpha_2 v_2(t_{k-1}) \end{aligned} \tag{15}$$

where μ_1 and μ_2 can be naturally replaced by 2; $\alpha 1$, $\alpha 2$ can be set to 1, and $F_1(t_k) = x_e^{(2)}(t_k) - v_1(t_{k-1})$, $F_2(t_k) = y_e^{(2)}(t_k) - v_2(t_{k-1})$. Finally, (15) is inverted and merged with (12) in the final i-PD feedback controller

$$\begin{aligned} v_1 &= \ddot{x}_r - F_1 + K_{P_x}e_x + K_{D_x}\dot{e}_x \\ v_2 &= \ddot{y}_r - F_2 + K_{P_y}e_y + K_{D_y}\dot{e}_y \end{aligned} \tag{16}$$

with the following:

- x_r and y_r the reference docking path;
- $e_x = x - x_r$ and $e_y = y - y_r$ the longitudinal and lateral tracking errors;
- K_{P_x}, K_{D_x}, K_{P_y}, and K_{D_y}, suitable PD controller gains.

Note that this approach needs derivatives estimates of noisy signals. A fast and robust technique, independent of noises' statistic properties has been used in this work (see [30] for more details).

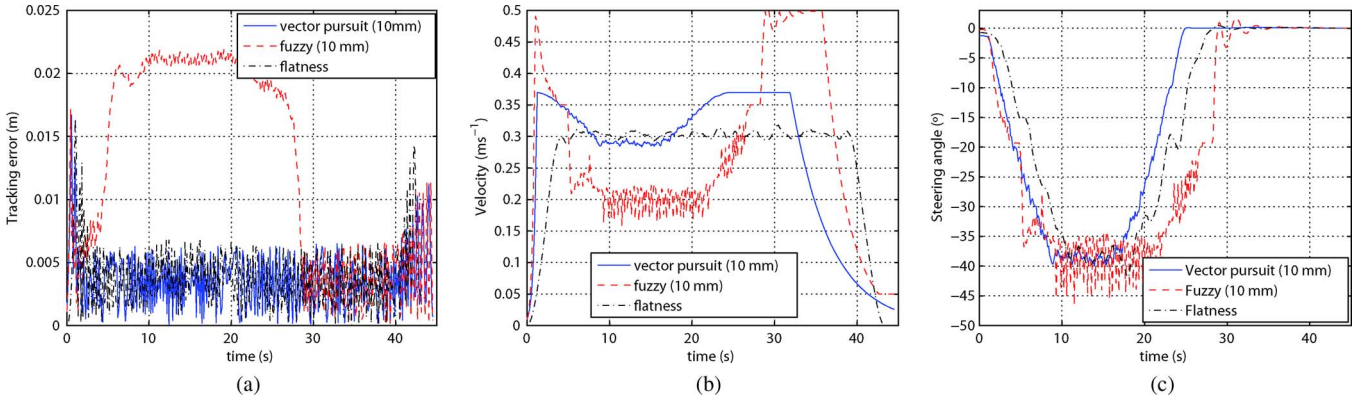

Fig. 4. Comparison between fuzzy, vector pursuit, and flatness-based controllers: (a) tracking error, (b) longitudinal velocity, and (c) steering angle.

V. Simulation Results and Robustness Analysis

The two non-model-based techniques previously described will be compared to the i-PD flatness based controller. In a first step, tracking quality and softness of movement will be analyzed for fuzzy, vector pursuit, and flatness-based controller (see Section V-A). Since the latter is based on a kinematic model of the AGV, not only good tracking performance will be sought, but also robustness to parameter uncertainty of model (3), (4). As a result, robustness of the intelligent flatness based controller will be afterwards evaluated using exhaustive Monte Carlo simulations (see Section V-B).

A continuous curvature path respecting a maximum allowable steering angle $\phi = \pm 60°$ (see Fig. 3) will be used to simulate the AGV behavior in a docking maneuver. Besides, a velocity profile (see [21] for more details) will be used to cover the whole path at a maximum speed $\dot{\sigma}_{\max} = 0.3\ \text{ms}^{-1}$ and with a maximum acceleration $\gamma_{x_{\max}} = 0.1\ \text{ms}^{-2}$. These constraints may seem too conservative, but current AGVs [31] operate at similar speeds in docking maneuvers due to industry regulation.

Note that the combination of such geometric path and velocity profile leads to steering angle evolution where constraints on steering angle and velocity ($\dot{\phi} = \pm 24°/\text{s}$) are fulfilled.

Position estimations of the navigation system are only available once per second and odometry sampling rate is constrained by control cycle duration ($T_s = 0.111$ s). Both values are merged in an extended Kalman filter (EKF), where measurement noises have to be characterized. In all the below simulations, wheel angular velocities are supposed to be corrupted with an additive white Gaussian noise $\mathcal{N}(0, \varsigma)$ whose standard deviation is $\varsigma = 10^{-3}$.

We assume that docking operation imposes a maximum error of 2 cm in the docking point positioning because it is where the load is located. We also assume that tracking error cannot exceed 10 cm during the docking maneuver because higher position errors may induce collisions. The third condition will be imposed to limit the effects of vibrations in the control of AGV and the load: the median of the steering angle fast Fourier transform (FFT) should not be higher than 0.02 Hz.

A. Non-Model Versus Model-Based Controllers

Fuzzy and vector pursuit control methods are not based on a vector profile, but rather on a maximum velocity. Thus, acceleration and deceleration phases have been configured to obtain a similar docking time than that obtained with flatness based control.

Since the two non-model based controllers are extremely sensitive to look-ahead distance, several choices (3, 5, and 10 cm) have been tested in order to obtain the best solution of each technique. In Table II all these configurations are compared to flatness based control in terms of tracking error (mean, maximum and final values) and softness of control actions (median value of the steering angle FFT). Note that these first results have been obtained with noisy measurements from a pure kinematic model.

We have noticed that, even though final and maximum values of tracking error are pretty similar for all techniques, the configurations that most reduce the effect of vibrations are those using a look-ahead distance of 10 cm. Consequently, only the latter configuration has been plotted in Fig. 4. Some conclusions can be highlighted from these results and confirmed with Table II:

- fuzzy controllers are significantly less precise and exhibit a more abrupt behavior than the other control approaches;
- tracking error obtained with vector pursuit control largely fulfills the aforementioned constraints and it acts in a softer way than fuzzy control. However, velocity profile is far from having a predictable shape;
- flatness-based controller provides a steering angle FFT median three times lower than the best fuzzy and vector pursuit implementations.

B. Flatness-Based Controllers

In a first step, the flatness-based feedback control is applied to a pure kinematic model (1). The blue curve in Fig. 5(a) shows that the tracking error is really reduced in these conditions.

Moreover, jerk variations will be also observed in order to estimate the amount of material that can be safely handled. In Fig. 5(b) and (c), control actions are plotted to give an insight of this sort of "transportability" indicator. Both velocity and steering angle exhibit a very smooth behavior.

Considering now that the model of (3) with skidding and slipping effects (or, in other words, with very different load and friction conditions) is used. Besides, the actuator dynamics described in (4) are also taken into account with the nominal values

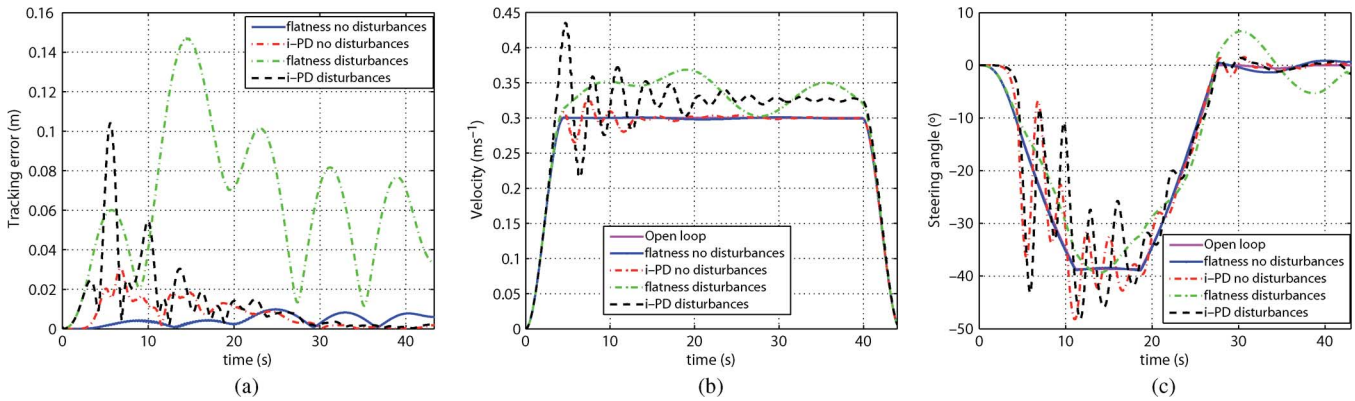

Fig. 5. Comparison between pure and intelligent flatness-based controllers: (a) tracking error, (b) longitudinal velocity, and (c) steering angle.

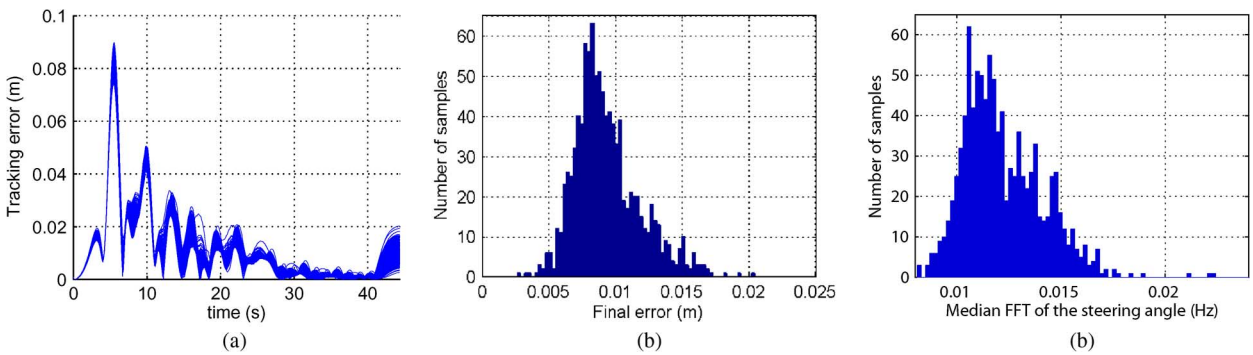

Fig. 6. Monte Carlo simulations: (a) tracking error, (b) final error histogram, (c) and histogram with the median of the steering angle FFT.

TABLE I
NOMINAL VALUES OF THE SYSTEM

Parameter	Value
Velocity natural frequency (ω_v)	50
Velocity damping ratio (η_v)	0.5
Velocity dead time (τ_v)	0.05
Skidding static gain (K_s)	0.01
Skidding natural frequency (ω_s)	10
Skidding damping ratio (η_s)	0.7
Steering static gain (K_ϕ)	10
Steering natural frequency (ω_ϕ)	20
Slip velocity ratio (τ)	0.05

TABLE II
COMPARISON OF CONTROLLERS

Controller	St. ang. FFT median (Hz)	Tracking error (m)		
		mean	max	final
Fuzzy (3 cm)	0.4935	0.0068	0.0164	0.0085
Fuzzy (5 cm)	0.4631	0.0081	0.0160	0.0108
Fuzzy (10 cm)	0.1902	0.0127	0.0219	0.0004
Vect. pursuit (3 cm)	0.1594	0.0025	0.0171	0.0050
Vect. pursuit (5 cm)	0.0892	0.0036	0.0162	0.0097
Vect. pursuit (10 cm)	0.0386	0.0036	0.0167	0.0007
Flatness	0.0137	0.0039	0.0164	0.0022

of Table I. Fig. 5 permits observing how difficult is to track the desired path with the flatness based controller when these disturbances are considered (red line). However, when the i-PD feedback control is applied to the same benchmark, a remarkable improvement is obtained (the 2 cm final error bound is widely respected).

It is then clear that the introduction of an "intelligent" feedback control considerably enhance the system robustness and stability domain while remaining within the desired smoothness ranges of the robot motion.

1) Robustness Analysis: As previously mentioned, the tracking quality will be evaluated under different load and friction conditions, and variable low level dynamics. In order to account for parametric uncertainty, we define the model's parameters as distributions of values rather than as single fixed values. We then perform a Monte Carlo simulation, running the model repeatedly with 1000 random combinations of parameter values. The parameters p_i in Table I will be considered to follow centered normal distributions of the form $\mathcal{N}(\mu_i, \sigma_i)$, $\mu_i = p_i$, $\sigma_i = 0.05\mu_i$.

Note that the Monte Carlo simulations were designed to take into account most of unknown or badly-known dynamics and parameters that have been traditionally neglected in the related literature. The analyzed parameter uncertainty space is wide enough to assume that there should not be a substantial difference between simulation and experimental closed-loop behavior.

After these 1000 random simulations, only 3 configurations did not fulfill the 3 constraints above enumerated. Moreover, as it can be appreciated in Fig. 6(a), only one among these faulty cases is due to a final error excess.

Fig. 6(b) and (c) show histograms of final tracking errors and medians of the steering angle FFT with the i-PD feedback controller. These two charts confirm the following:

- a remarkable tracking quality for a model-based controller under a high degree of uncertainty;
- an acceptable level of transportability when compared to non-model based controllers-even if high amplitude variations in steering angle can be observed in Fig. 5, its FFT histogram show that their frequencies are tolerable.

To sum up, note that i-PD controller compensates skidding, slipping and actuators dynamics without need of physical parameter or supplementary measure.

VI. Concluding Remarks

This work has presented a comparison in depth between different control approaches for AGV robust path tracking. The compared control strategies seek to ensure low jerk variations in docking operations of AGVs in industrial environments. The proposed control system is focused on the one hand on robustness and performance (slight errors can damage the load or the station), and on the other hand on ease configuration of the controller (a reduced set of parameters should be enough to easily adapt to new layouts or production rates).

Two non-model-based control techniques (fuzzy and vector pursuit) have been confronted to a new nonlinear model-based control strategy. In the latter, a data-driven model for robust feedback control has been combined with differential flatness to obtain a control strategy, specially well suited for AGV path tracking in industrial environments. The simulations have shown very interesting results with no need of physical parameters knowledge and with a high degree of efficiency.

References

[1] H. Martínez-Barberá and D. Herrero-Pérez, "Development of a flexible AGV for flexible manufacturing systems," *Ind. Robot*, vol. 37, no. 5, pp. 459–468, 2010.

[2] H. Martínez-Barberá and D. Herrero-Pérez, "Autonomous navigation of an automated guided vehicle in industrial environments," *Rob. Comput. Integr. Manuf.*, vol. 26, no. 4, pp. 296–311, 2010.

[3] B. Siciliano and O. Khatib, *Springer Handbook of Robotics*. New York: Springer-Verlag, 2008.

[4] T. Das and I. N. Kar, "Design and implementation of an adaptive fuzzy logic based controller for wheeled mobile robots," *IEEE Trans. Control Syst. Technol.*, vol. 14, no. 3, pp. 501–510, May 2006.

[5] K. R. S. Kodagoda, W. S. Wijesoma, and E. K. Teoh, "Fuzzy speed and steering control of an AGV," *IEEE Trans. Control Syst. Technol.*, vol. 10, no. 1, pp. 112–120, Jan. 2002.

[6] R. Fierro and F. L. Lewis, "Control of a nonholonomic mobile robot: Backstepping kinematics into dynamics," *J. Robotic Syst.*, vol. 14, no. 3, pp. 149–163, 1997.

[7] Y. J. Lee, J. H. Suh, J. W. Lee, and K. S. Lee, "Driving control of an AGV for an automated container terminal using an immunized PID controller based on cell-mediated immunity," *Artif. Life Robot.*, vol. 9, no. 2, pp. 90–95, 2005.

[8] J. S. Wit, C. Crane, and D. Armstrong, "Autonomous ground vehicle path tracking," *J. Robot. Syst.*, vol. 21, no. 8, pp. 439–449, 2004.

[9] C. Canudas de Witt, G. Bastin, and B. Siciliano, *Theory of Robot Control*. New York: Springer-Verlag, 1996.

[10] W. Dong and W. Huo, "Tracking control of wheeled mobile robots with unknown dynamics," in *Proc. IEEE Int. Conf. Robot. Autom.*, 1999, pp. 2645–2650.

[11] T. Fukao, H. Nakagawa, and N. Adachi, "Adaptive tracking control of a nonholonomic mobile robot," *IEEE Trans. Robot. Autom.*, vol. 16, no. 5, pp. 609–615, Oct. 2000.

[12] F. N. Martins, W. C. Celeste, R. Carelli, M. Sarcinelli-Filho, and T. F. Bastos-Filho, "An adaptive dynamic controller for autonomous mobile robot trajectory tracking," *Control Eng. Pract.*, vol. 16, no. 11, pp. 1354–1363, 2008.

[13] B. d'Andréa-Novel, G. Campion, and G. Bastin, "Control of nonholonomic wheeled mobile robots by state feedback linearization," *Int. J. Robot. Res.*, vol. 14, no. 6, pp. 543–559, 1995.

[14] M. L. Corradini, T. Leo, and G. Orlanndo, "Experimental testing of a discrete-time sliding mode controller for trajectory tracking of a wheeled mobile robot in the presence of skidding effects," *J. Robot. Syst.*, vol. 19, no. 4, pp. 177–188, 2002.

[15] A. P. Aguiar and J. P. Hespanha, "Trajectory-tracking and path-following of underactuated autonomous vehicles with parametric modeling uncertainty," *IEEE Trans. Autom. Control*, vol. 52, no. 8, pp. 1362–1379, Aug. 2007.

[16] M. Fliess, J. Lévine, P. Martin, and P. Rouchon, "Flatness and defect of nonlinear systems: Introductory theory and examples," *Int. J. Control*, vol. 61, no. 6, pp. 1327–1361, 1995.

[17] M. Defoort, J. Palos, A. Kokosy, T. Floquet, W. Perruquetti, and D. Boulinguez, "Experimental motion planning and control for an autonomous nonholonomic mobile robot," in *Proc. IEEE Int. Conf. Robot. Autom.*, 2007, pp. 2221–2226.

[18] D. Buccieri, D. Perritaz, P. Mullhaupt, Z. P. Jiang, and D. Bonvin, "Velocity-scheduling control for a unicycle mobile robot: Theory and experiments," *IEEE Trans. Robot.*, vol. 25, no. 2, pp. 451–458, Apr. 2009.

[19] C. B. Low and D. Wang, "GPS-based tracking control for a car-like wheeled mobile robot with skidding and slipping," *IEEE/ASME Trans. Mechatron.*, vol. 13, no. 4, pp. 480–484, Aug. 2008.

[20] P. Rouchon, M. Fliess, J. Lévine, and P. Martin, "Flatness and motion planning: The car with n trailers," in *Proc. Euro. Control Conf.*, Groningen, The Netherlands, 1993, pp. 1518–1522.

[21] J. Villagra, D. Herrero-Pérez, and M. Abderrahim, "Robust flatness-based control of an AGV under varying load and friction conditions," in *Proc. IEEE Conf. Control Autom.*, 2009, pp. 1621–1628.

[22] G. Genta, *Motor Vehicle Dynamics: Modeling and Simulation*, ser. Series on Advances in Mathematics for Applied Sciences. Singapore: World Scientific, 1997, vol. 43.

[23] D. Wang and C. B. Low, "Modeling and analysis of skidding and slipping in wheeled mobile robots: Control design perspective," *IEEE Trans. Robot.*, vol. 24, no. 3, pp. 676–687, Jun. 2008.

[24] B. Siciliano, L. Sciavicco, L. Villani, and G. Oriolo, *Robotics: Modelling, Planning, and Control*. New York: Springer, 2009.

[25] F. Hoffmann, "Evolutionary algorithms for fuzzy control system design," *Proc. IEEE*, vol. 89, no. 9, pp. 1318–1333, Sep. 2001.

[26] E. H. Mamdani and S. Assilian, "An experiment in linguistic synthesis with a fuzzy logic controller," *Int. J. Man Mach. Stud.*, vol. 7, no. 1, pp. 1–13, 1975.

[27] M. Fliess, J. Lévine, P. Martin, and P. Rouchon, "Design of trajectory stabilizing feedback for driftless flat systems," in *Proc. Eur. Control Conf.*, 1995, pp. 1882–1887.

[28] M. Fliess and C. Join, "Intelligent PID controllers," in *Proc. Med. Conf. Control Autom.*, 2008, pp. 326–331.

[29] M. Fliess and C. Join, "Commande sans modèle et commande à modèle restreint," *e-STA*, vol. 5, no. 4, pp. 1–23, 2008.

[30] M. Mboup, C. Join, and M. Fliess, "Numerical differentiation with annihilators in noisy environment," *Numer. Algorithms*, vol. 50, no. 4, pp. 439–467, 2009.

[31] D. Herrero-Pérez and H. Martínez-Barberá, "Modeling distributed transportation systems composed of flexible automated guided vehicles in flexible manufacturing systems," *IEEE Trans. Ind. Inf.*, vol. 6, no. 2, pp. 166–180, May 2010.